Measurements of a Krypton Fed 1.5 kW Hall Effect Thruster with a Centrally Located Cathode

IEPC-2017-26

Presented at the 35th International Electric Propulsion Conference,
Georgia Institute of Technology • Atlanta, GA • USA
October 8 - 12, 2017

James Szabo* Rachel Tedrake,† George Kolencik,‡ Bruce Pote§
Busek Co. Inc, Natick, MA, 01760, USA

A 1.5 kW laboratory model Hall Effect thruster designed for xenon was tested with krypton propellant. The cathode was located along the central axis of the thruster, and was also fueled by krypton. Thrust was measured with an inverted pendulum stand. Ion plume current was measured with a nude Faraday probe. Discharge power varied from 1.1 to 2.5 kW, while discharge potential varied from 200 to 600 V. Presented test results include measurements of thrust, specific impulse, and efficiency as a function of power, flow rate, and discharge potential. Plots of ion plume current as a function of angular position are also presented. Specific impulse was higher with krypton than with xenon, but efficiency was significantly lower. The plume shape was relatively invariant with thruster operating conditions, and was more divergent with krypton than with xenon. Test results are analyzed from a theoretical standpoint, and the merits of krypton are discussed.

Nomenclature

$\vec{B}$	=	magnetic field
$\vec{E}$	=	electric field
e	=	charge of an electron, 1.6 x 10^{-19} C
g_0	=	gravitational constant at Earth's surface, 9.81 m/s^2
I	=	current
I_{sp}	=	specific impulse
j	=	current density
L	=	characteristic length
λ_i	=	mean free path for neutral to be ionized
$\dot{m}$	=	mass flow rate, subscripts a for anode, c for cathode
M	=	ion mass
P_d	=	discharge power
p	=	probability of ionization
T	=	thrust
V_d	=	discharge potential
η	=	efficiency

* Chief Scientist for Hall Thrusters, jszabo@busek.com
† Research Engineer, rachel@busek.com
‡ Research Engineer, george@busek.com
§ Director, Hall Thrusters, bpote@busek.com

I. Introduction

The Hall Effect Thruster (HET) is an efficient form of spacecraft electric propulsion that may be used for orbit raising, orbit maintenance, and other applications. This paper presents thruster performance and plume measurements taken with a krypton (Kr) fueled HET where the cathode is located along the geometrical thruster axis. Xenon data are presented for comparison.

A. Hall Thruster Theory

HETs use crossed electric and magnetic fields to generate and accelerate ions. The overall structure of the device tested here is defined by a magnetic circuit that produces a steady magnetic field $\vec{B}$, in the nominal radial direction across an annular discharge channel. Neutral propellant is introduced at the upstream portion of the channel. A potential difference is applied between the gas distributor, which acts as the anode, and a cathode located outside the channel. The downstream portion of the channel is dielectric. Most cathode electrons flow to the plume, but some flow into the channel, seeding the plasma discharge, which is driven by electron impact ionization. The electric field, $\vec{E}$, is predominantly axial and is concentrated near the channel exit by interactions between the magnetic field and the plasma. Because electrons are strongly magnetized, local transport is predominantly azimuthal due to the eponymous $\vec{E}\times\vec{B}$ Hall Effect. Figure 1 is a notional thruster cross-section where the cathode is located central to the main plasma discharge. The cathode may also be located external or distal to the discharge channel.

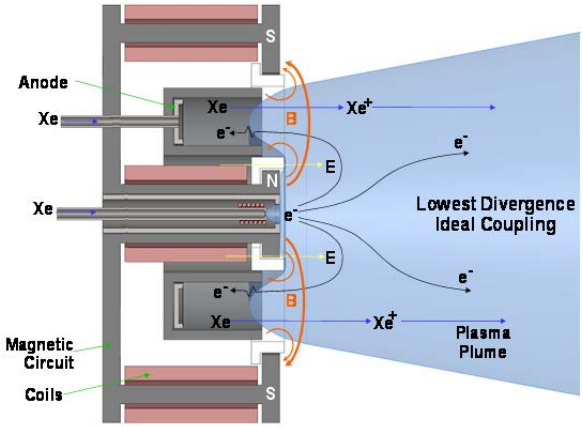

Figure 1. Axisymmetric Hall Effect Thruster geometry with center mounted cathode.

Discharge power, P_d is the product of discharge voltage, V_d, and discharge current, I_d. Total thruster power also includes power used to drive the magnetic circuit and power used to start and maintain the cathode. The latter includes power to the cathode heater and power to the cathode keeper.

The fraction of the propellant which becomes ionized is an important determinant of thruster performance. If the thickness of the ionization layer is given by L, then the probability of ionizing a neutral as it passes through the layer is given by Eq. 1.[1,2]

$$p = 1 - \exp(-L/\lambda_i) \tag{1}$$

Here, λ_i is the mean free path for ionizing collisions, which is a function of plasma density, neutral speed, electron temperature and the ionization cross section. If L/λ_i =3, then p =95%.

Ions are weakly magnetized and most are accelerated downstream, forming the ion beam. The plume is not well collimated, and the ion current density, j, decays exponentially as the angle, θ, from the plume axis increases. Some ions may flow to the channel wall, sputtering the channel. Sputter rate varies with ion energy, ion flux, angle of incidence and other factors.

B. Krypton and Other Propellants

The first HET in space was a Soviet Stationary Plasma Thruster (SPT) launched in 1971 aboard the Meteor-18 spacecraft.[3] The first American HET to fly in space was the Busek BHT-200, which was launched in 2006 as part of the TacSat-2 spacecraft.[4] Both of these thrusters were fueled by xenon (Xe), which is inert, heavy, and easy to ionize.

Many other substances may be used to fuel a Hall thruster, yielding sundry benefits such as lower propellant cost, higher storage density, and higher specific impulse. The catalog of alternate propellants includes, among others, krypton, iodine (I), and bismuth (Bi). Table 1 contains properties of krypton, iodine, xenon, and bismuth related to ionization and propellant storage.

Iodine is easy to ionize, has an atomic mass similar to that of xenon, and stores in the solid phase at roughly three times the density of high pressure xenon. In performance testing at widely disparate power levels, little or no performance penalty has been observed.[5,6] However, iodine reactivity presents multiple engineering challenges.

Bismuth is also easy to ionize and is much heavier than xenon or iodine, with potential benefits for missions requiring high thrust to power. Like iodine, bismuth stores at high density in a condensed phase feed system, and high efficiency is observed before ancillary power losses are considered.[7,8] However, the vapor pressure of bismuth is very low, necessitating the use of high power heaters (representing a parasitic power loss) to prevent condensation and deposition. This is especially important during thruster start-up.

Table 1. Properties of Kr, I, Xe, and Bi.[9, 10,11,12,]

Element	Kr	I	Xe	Bi
Atomic Mass	83.8	126.9	131.3	209.0
Ionization Properties (monatomic)				
First Ionization Potential (eV)	14	10.5	12.1	7.3
Peak Cross Section (10^{-16} cm^2)	3.7	6.0	4.8	8.0
Storage and Handling Properties				
Storage density (gm/cm^3) near room temp.	0.53*	4.9	1.6*	9.8
Melting Point (^oC)	-157	113.7	-112	271
Boiling Point at 10 Pa (^oC)	-208	9	-181	768

*14 Mpa, 50 C (NIST Database)

From a system standpoint, the noble gas krypton is most like xenon, allowing the use of thruster, cathode, and feed system components originally developed for xenon. Krypton is also less expensive than xenon. Furthermore, krypton is lighter than xenon, enabling higher specific impulse at the same discharge potential.

To its detriment, krypton stores at much lower density than iodine, xenon, and bismuth. At 14 MPa and 50^o C (which may be considered typical conditions), the stored density of krypton is one third that of xenon. Welle has shown that there is an optimum storage pressure for Kr and Xe, where deviations exact a significant mass penalty; for a spherical titanium tank, the optimal density for Kr is 0.8 g/cc at 17.9 MPa.[13] However, the stored density of Kr increases dramatically as temperature is reduced. At -50^o C, stored density of krypton is comparable to xenon at 50^o C. Figure 2 plots krypton density as a function of pressure at -50^o C, 0^o C, and 50^o C.

Also to its detriment, krypton is harder to ionize than xenon, iodine, and bismuth, leading to lower propellant utilization and thruster efficiency. This is because the mean free path for ionizing collisions, λ_i , is relatively large. Contributing factors include the light weight of the neutrals (which makes them fast), relatively high ionization energies, and relatively small ionization cross sections. Figure 3 illustrates the relative magnitude of the electron impact ionization cross sections for krypton and xenon.

Krypton has been previously tested with multiple medium and low power Hall thrusters such as the BHT-600,[14,15] SPT-100,[16,17,18] ATON,[19] and NASA-173Mv1[20, 21] all of which have external cathodes. These studies found that replacing xenon with krypton exacted a significant performance penalty, and that efficiency was maximized by running at high power, flow rate and discharge voltage.

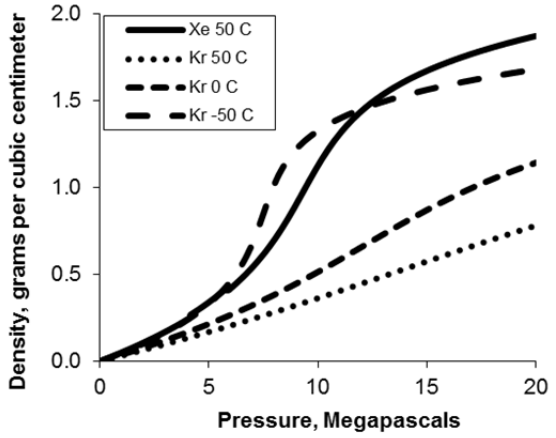

Figure 2. Stored density of krypton and xenon at high pressure.

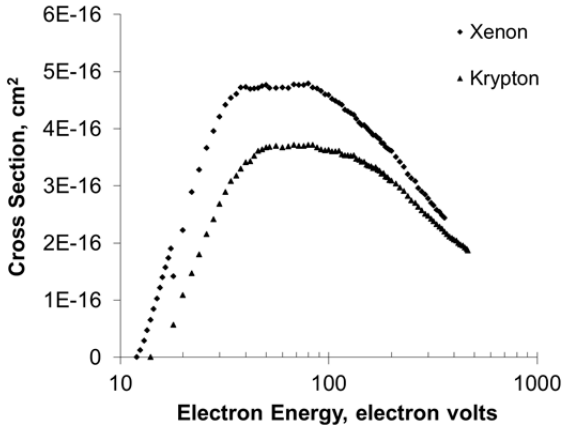

Figure 3. Krypton and xenon electron impact cross sections for single ionization.[10]

Krypton has also been tested with the large NASA-457 M thruster, which has a center cathode, at power levels up to 72.5 kW. With this thruster, NASA researchers found an insignificant difference in efficiency at equivalent number flow rates (SCCM) for krypton and xenon.[22] This may be the consequence of $L / \lambda_i >> 1$.

Some studies indicate that krypton performance may be improved by adopting a modified magnetic field topology.[18,21] However, the thruster used in the present study (the BHT-1500-C) was changed in no way from the xenon configuration.

C. Benefits of Center Cathode

Studies of the multiple thrusters have shown that the center cathode position is optimal for thruster performance and plume divergence.[23] Studies have also shown that the performance of thrusters where the cathode is externally mounted may be artificially inflated by facility effects associated with high background pressure, and that this inflation is minimal or non-existent when the cathode is mounted along the thruster central axis.

A detailed study of background pressure effects was conducted with Busek's qualification model BHT-1500-E flowing xenon at the Aerospace Corporation in El Segundo, CA.[24] Performance was studied both with the cathode along the centerline, and with the cathode external to the discharge. Background pressure spanned approximately a decade (6 x 10^{-6} Torr to 4 x 10^{-5} Torr). Data were taken at multiple operating conditions: (P_d, V_d) = (1.8 kW, 300 V), (1.5 kW, 300 V), (1.8 kW, 400 V), and (1.5 kW, 400 V). Aerospace researchers found that center-mounting the cathode improved performance, reduced plume divergence, and reduced the amount of cathode flow necessary to maintain efficient operation. More significant for the present krypton study, performance was relatively insensitive to chamber background pressure when the cathode was center mounted. When background pressure was increased by a factor of 10, Aerospace researchers measured little difference in efficiency and only a small change in specific impulse. When the cathode was mounted externally, efficiency increased significantly with background pressure. Some of the efficiency and specific impulse data are plotted in Figure 4.

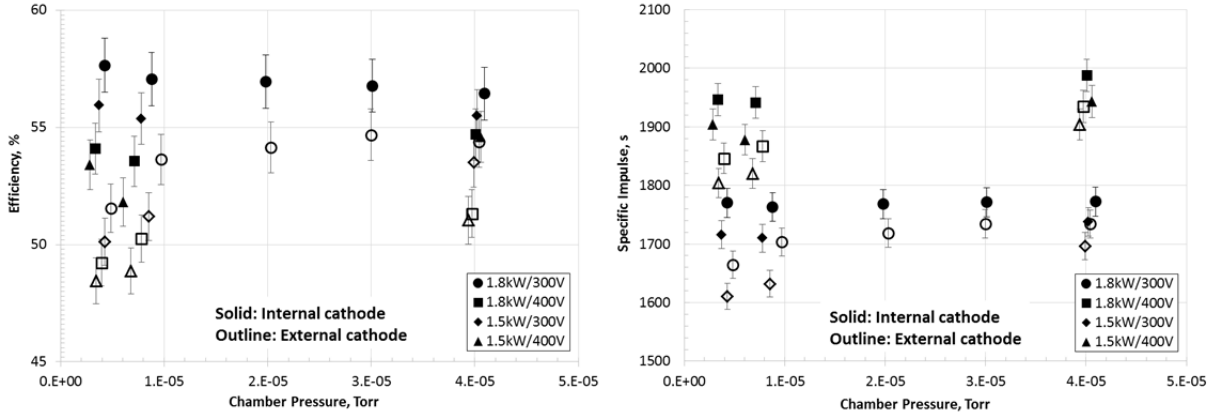

Figure 4. Effect of cathode position upon thruster performance (data from Ref. 24).

Aerospace researchers also observed strong sensitivity to background pressure with the SPT-100, which has an external cathode.[25] Similar effects were observed at the Air Force Research Laboratory (AFRL) with Busek's laboratory model BHT-600, which also has an external cathode, although less sensitivity to background pressure was measured with krypton than with xenon.[15]

Krypton test data reported in the literature fall into one of three categories. In the first category, the cathode was mounted externally, but the data were taken when the background pressure was low, muting the impact of cathode position upon performance. For instance, when the NASA-173Mv1 data of Ref. 20 were taken, the chamber pressure was 3 x 10^{-6} Torr. Similarly, when the BHT-600 data of Ref. 14 were taken, the chamber pressure was 7 x 10^{-6} Torr. In the second category, the cathode was mounted externally and the background pressure was high enough to significantly impact (i.e. improve) thruster performance. For instance, the SPT-100 data of Ref. 16 were taken at a chamber pressure of 2 x 10^{-5} Torr, while the ATON thruster data of Ref. 19 were taken at a background pressure of 10^{-4} Torr. In the third category, the background pressure was relatively high, but the cathode was mounted externally, which means the measurements are largely representative of in-space performance. Krypton data taken with the NASA-457M fall into this category because the chamber pressure peaked at 2 x 10^{-5} Torr.[22] The

krypton data reported in this paper also fall into this category because the chamber pressure was 2.5 – 6.1 x 10^{-5} Torr.

II. Apparatus and Procedure

A. BHT-1500 Thruster and Center Cathode

The BHT-1500 is an annular thruster designed to operate at a nominal power level of 1500 W. The mean diameter of the discharge cavity is 82 mm. The design features a patented anode assembly which passively shunts a portion of the magnetic field, creating a magnetic lens with steep axial gradient and near zero |B| close the anode. The downstream portion of the discharge channel is lined with a boron nitride composite.

The first thruster called BHT-1500 was a laboratory model developed for high voltage operation.[26] The cathode was external to the discharge channel, as shown in Figure 5 (left). Reported work included performance mapping, plasma modeling, and detailed plume studies at various background conditions.[2,27,28,29] Performance was found to be competitive with the NSTAR ion engine, with peak specific impulse exceeding 3000 s and peak anode efficiency exceeding 60%. A laboratory model BHT-1500 was delivered to the NASA Glenn Research Center (GRC) circa 2004.

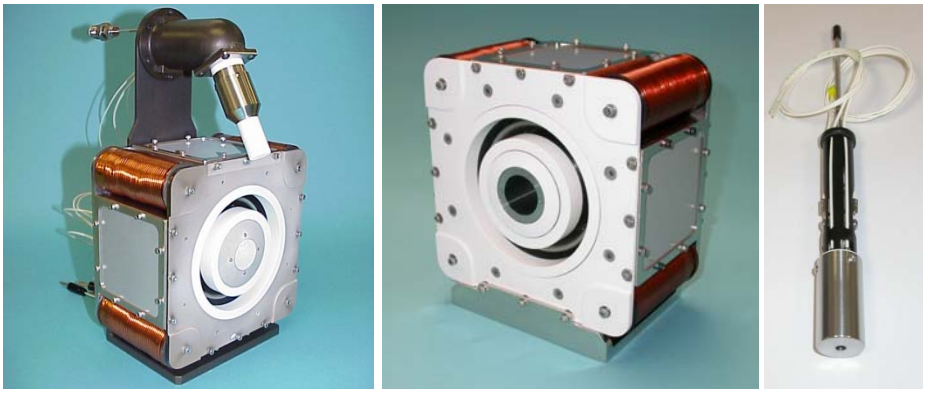

Figure 5. BHT-1500 (left), BHT-1500-C (middle), and BHC-2500 laboratory model cathode (right).

In 2008, the BHT-1500 laboratory model was redesigned to locate the cathode along the geometrical thruster axis. The revised thruster, known as the BHT-1500-C, was used to take the krypton measurements reported in this paper. A BHT-1500-C was also delivered to the Air Force Institute of Technology (AFIT), where it was studied with xenon.[30] The BHT-1500-C is shown in Figure 5 (middle) along with the laboratory model BHC-2500 cathode which was used for the testing reported in this paper.

The BHC-2500 cathode uses a porous tungsten hollow insert impregnated with a low work function electron emitter comprised of a barium-calcium-aluminate mixture in a tungsten matrix. A resistive heating element brings the cathode to ignition temperatures. A keeper electrode is used to start the cathode discharge. When a thruster discharge is present, the cathode will operate without the heater or keeper discharge. In any case, the flow rate of propellant is typically 5 - 10% of the anode mass flow rate.

The BHT-1500-E which was tested at the Aerospace Corporation is the qualification model of the BHT-1500-C. It retains all critical features of the BHT-1500-C including a center-mounted cathode.[24] The BHT-1500-E also has an improved magnetic field shape which reduces channel erosion and increases thruster lifetime.

B. Facilities

To accurately measure performance, the background pressure must be low enough that it does not significantly affect the plasma processes or feed the discharge background neutrals. To achieve such a space-like environment, the thruster was performance tested in Busek's cryogenically-pumped T8 vacuum chamber, which has a nominal xenon pumping speed of 200,000-l/s. This facility has a diameter of 2.4-m and a length of 5-m. Background pressure was measured with an ion gauge located on the wall of the facility. Measured pressure was corrected for krypton using standard calibration factors.

C. Performance Measurements and Metrics

The thruster was powered by manually regulated laboratory power supplies from Sorensen and Universal Voltronics. The thruster-cathode system was electrically isolated from facility ground, as is representative of in-space operation. The inner and outer solenoid circuits were driven by separate DC power supplies independent of the discharge. Figure 6 is a nominal power supply diagram.

Thrust, T, was measured with a calibrated inverted pendulum thrust stand.[31] During testing, the thrust stand was periodically re-zeroed to minimize uncertainty.

Propellant flow was regulated by flow controllers sourced from Unit Instruments. Both the thruster and cathode were fueled by the same propellant. That is, when the thruster was fueled by krypton, the cathode was also fueled by krypton. The ratio of cathode to anode flow rate was maintained at $\dot{m}_c / \dot{m}_a$ =10%.

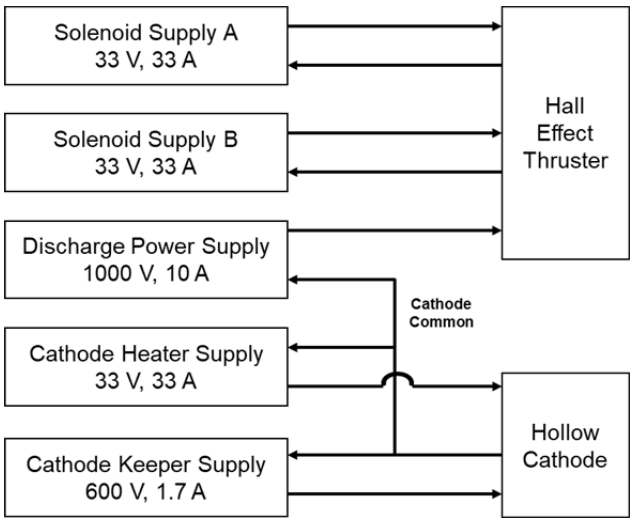

Figure 6. Nominal power supply diagram.

Specific impulse was calculated from thrust, mass flow rate, and the gravitational constant at Earth's surface, g_0:

$$I_{sp} = T / \dot{m} g_0 . \tag{2}$$

Ignoring facility effects, mass flow rate, $\dot{m}$, is the sum of the anode mass flow rate, $\dot{m}_a$, and the cathode mass flow rate, $\dot{m}_c$. Anode I_{sp} was calculated with $\dot{m}_a$ only, excluding cathode flow.

Total thruster efficiency, η, was calculated from thrust, mass flow rate, and power:

$$\eta = T^2 / 2\dot{m} P . \tag{3}$$

Anode efficiency, η_a, was calculated with $\dot{m}_a$ and P_d only, excluding cathode flow, cathode power, and solenoid power.

Efficiency and specific impulse are related to thrust to power by

$$T / P = 2\eta / I_{sp} g_o . \tag{4}$$

When calculating η and I_{sp} from experimental data, the cathode flow fraction, $\dot{m}_{c/} \dot{m}_a$, was assumed to be 6.0% as opposed to the actual value of 10%. This allows a more direct comparison with data from Ref. 24.

D. Plume Measurements and Metrics

Plume current was measured with a Faraday probe originally designed by Azziz.[27,28,29] Key components of the probe include the collector and the guard ring, which shields the collector from low energy ions. The collector and guard ring are biased at the same potential to minimize edge effects. The probe was mounted on a rotary stage and swept across the exhaust beam centerline. The center of rotation was below the thruster exit, and the measured distance from the center of the thruster exit to the probe was 51.5 cm. The probe arm geometry is diagrammed in Figure 7.

Plume current density, j, was measured with a current shunt resistor and collected by an Agilent data acquisition system coupled to National Instruments' LabVIEW software. The plume current was, in some cases, scaled by the discharge current:

$$j_s = j(I_d / I_0) . \tag{5}$$

In this equation, j_s is the scaled current density, I_0 is the discharge current associated with j, and I_d = 4 A is discharge current to which the ion current density is scaled.

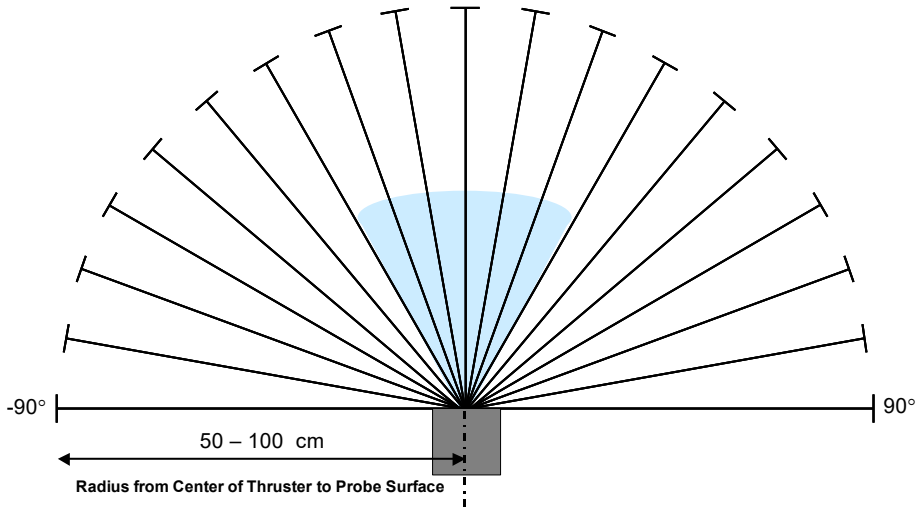

Figure 7. Far field plume measurement apparatus.

III. Results

A. Operation and Stability

The plasma discharge was stable with both krypton and xenon. With krypton, discharge stability was more sensitive to variations in the magnetic field strength, $|B|$, but lower field strength was required. This improved margin with respect to the peak field that could be generated by the thruster.

For both propellants, no additional heater power was supplied to the cathode after the thruster was started. Nevertheless, cathode floating potential was nearly the same with both propellants; for xenon, the range was -7 to -11 V, while for krypton the range was -8 to -12 V.

Unless otherwise indicated, all subsequent discussion of thruster performance and plume properties pertains to krypton.

B. Measured Performance

Testing focused on the power band $1.5 \leq P_d \leq 2.0$ kW, but also included some points outside that band. The discharge potential range was 200 V $\leq V_d \leq$ 600 V. Flow rates were chosen to yield similar operating conditions (I_d,V_d) with xenon and krypton; the anode flow rate, $\dot{m}_a$, was 42- 82 SCCM for the krypton test and 40 - 70 SCCM for the xenon test.

For krypton performance testing, chamber pressure was 2.5 - 6.1 x 10^{-5} Torr, after correcting for krypton. For xenon performance testing, chamber pressure was 1.0 – 1.5 10^{-5} Torr.

With krypton, measured T and I_{sp} increased with V_d. Peak I_{sp} exceeded 2000 s at V_d =400 V and 2500 s at V_d =600 V. Specific impulse also increased with $\dot{m}$ at constant V_d, an effect which may reflect higher propellant utilization. Figure 8 plots T and I_{sp} against V_d and $\dot{m}_a$.

With krypton, efficiency, η, increased with V_d at constant $\dot{m}_a$, and with $\dot{m}_a$ at constant V_d. The highest recorded efficiencies in the 1.5 – 2.0 kW power band occurred at V_d =300 - 400 V and $P_d \approx$ 2-kW, where η was almost 50%. Figure 9 plots η against V_d and $\dot{m}_a$.

In general, η increases with P_d. However, lower V_d at higher $\dot{m}$ was sometimes more efficient than higher V_d at lower $\dot{m}$. Figure 10 plots η against power, P.[**]

[**] Here, cathode keeper power was left out of the η calculation. The rationale is to provide a more consistent comparison between data points, since the keeper current was not constant during testing.

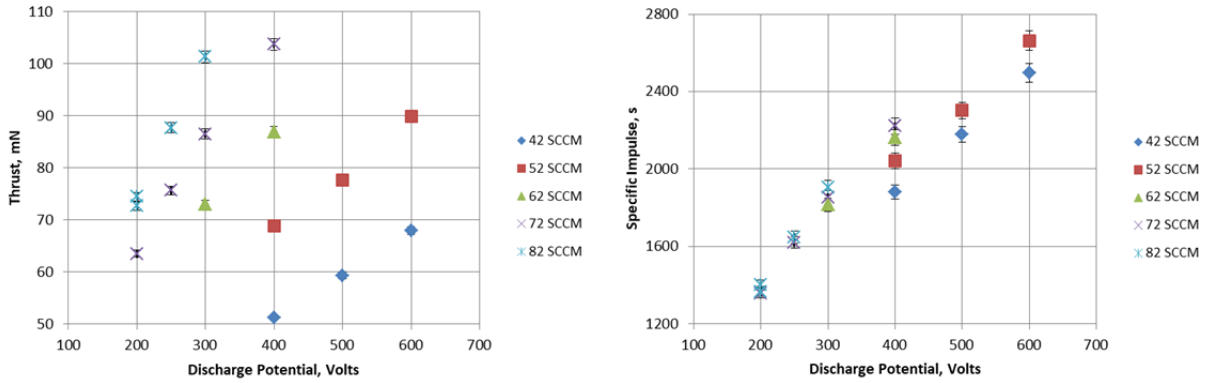

Figure 8. Thrust and specific impulse vs. discharge potential and anode flow rate (krypton).

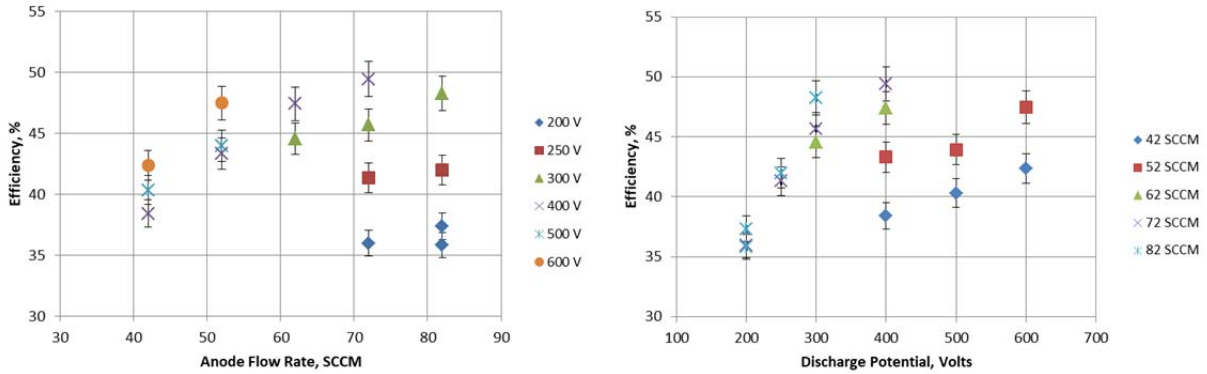

Figure 9. Efficiency vs. anode flow rate and discharge potential (krypton).

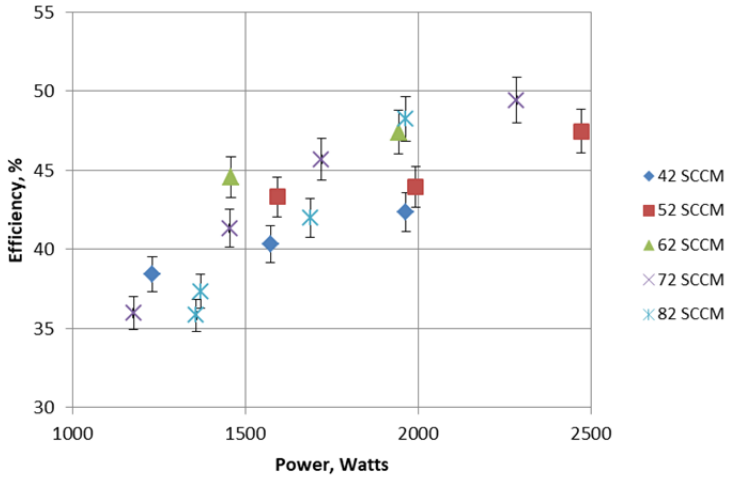

Figure 10. Thruster efficiency vs. power (krypton).

Thrust to power exceeding 50 mN/kW was available across a wide range of I_{sp}, which could be increased or decreased by varying the discharge potential. Curves of T/P vs. I_{sp} as a function of efficiency (Eq. 4) are plotted against krypton data in Figure 11.

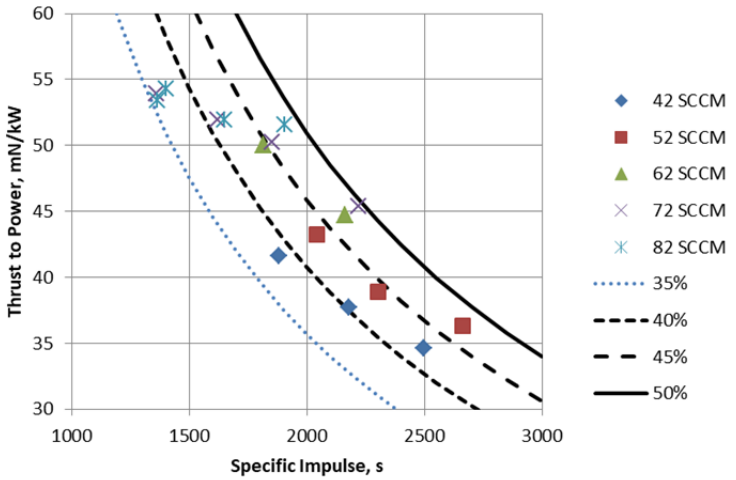

Figure 11. Curves of thrust to power ratio vs. specific impulse including experimental krypton data.

Xenon data were also taken, enabling a direct comparison between the two propellants. Per Table 2, the use of krypton increased specific impulse by approximately 140 – 190 s at nearly equivalent conditions (P_d, V_d). However, the use of krypton decreased efficiency by 7% to 8%.

Table 2. Performance of BHT-1500-C with xenon and krypton.

Thruster	Gas	Power (Watts)	Discharge Potential (Volts)	Anode Flow Rate (SCCM)	Specific Impulse (s)	Efficiency (%)	P Background* (Torr)
BHT-1500-C	Xe	1.6	300	60	1680	52.0	1.3E-05
		1.4	400	40	1890	51.5	1.1E-05
		1.9	300	70	1700	53.1	1.5E-05
		1.8	400	50	1970	54.3	1.0E-05
BHT-1500-C	Kr	1.5	300	62	1820	44.5	4.8E-05
		1.6	400	52	2040	43.3	4.6E-05
		1.7	300	72	1850	45.7	5.5E-05
		1.9	400	62	2160	47.4	5.1E-05

*Corrected for Kr where appropriate

The uncertainty associated with performance measurements was estimated with methods previously described for the BHT-1500 laboratory model.[26] The error bars shown on the figures are intended to represent one standard deviation; they are not absolute limits.

The normalized standard deviation, σ, or uncertainty in power, P, is estimated to be 1.1%. The principal source of uncertainty was the current measurement.

For krypton, the uncertainty in thrust, T, is estimated to be 1.1%; with contributions from the thrust stand calibration curve, sample-to-sample signal variation, and thrust stand signal drift. For xenon, the uncertainty in T is estimated to be 1.5%. Drift in the thrust stand zero was higher during the xenon test series.

The uncertainty in mass flow rate, $\dot{m}$, is estimated to be 1.5% for krypton and 1.0% for xenon, with contributions from the flow controller and neutral backflow from the facility. The flow controllers were assumed to be accurate to within 1%. To estimate neutral backflow, the krypton or xenon background pressure was assumed to be well represented by the indicated tank pressure, and the temperature of the background neutrals was assumed to be 300 K. Backflow thus calculated was as large as 1.1% of the metered flow rate for krypton and 0.3% of the metered flow rate for xenon. Backflow was only accounted for in the error bars and not in the base measurements.

For krypton, starting from uncertainties in P, T, and $\dot{m}$, the uncertainty in I_{sp} is estimated to be 1.9% and the uncertainty in η is estimated to be 2.9%. Thus, if I_{sp} =2000 s the error bar +/- 38 s. Likewise, if η = 40%, the error bar is +/- 1.2%. For xenon, estimated uncertainties in I_{sp} and η are 1.8% and 3.4%, respectively.

B. Measured Ion Current Density

The discharge plasma and near field plume of the BHT-1500-C operating on xenon and krypton is shown in Figure 12. Aside from the difference in color, the plume is visually similar with both propellants.

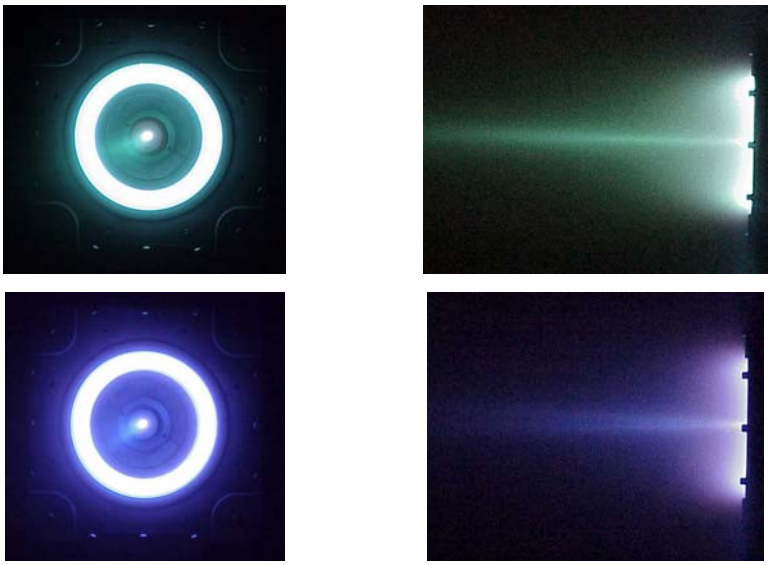

Figure 12. BHT-1500-C operating on xenon (top) and krypton (bottom).

Krypton faraday probe data are presented for discharge potentials from 300 V $\leq V_d \leq$ 600 V. Xenon data were also taken and are presented to provide a point of comparison. In general, the plume was highly symmetric. Measured plume current density at $V_d = 300$ V and 400 V is plotted in Figure 13.

After scaling by discharge current, the data at $V_d = 300$ V and 400 V collapse on top of each other. It is thus seen that increasing discharge power and beam utilization has little effect upon plume shape. It is also thus seen that higher background pressure associated with higher flow rate and discharge current has little effect upon the shape. Scaled plume current density at $V_d = 300$ V and 400 V is plotted in Figure 14.

Krypton data taken at different anode potentials also collapse on top of each other after normalization by discharge current. Scaled plume current density at 300 V – 600 V is plotted in Figure 15.

A comparison with the xenon plume shows that divergence is higher with krypton. Some of this difference could be the result of background pressure, which varied from 3.5 x 10^{-5} to 6.1 x 10^{-5} Torr in the krypton plume study, after correcting the pressure measurement for krypton. The xenon reference data were taken at 1.2 x 10^{-5} Torr. Scaled data for xenon and krypton at 300 V are plotted in Figure 16.

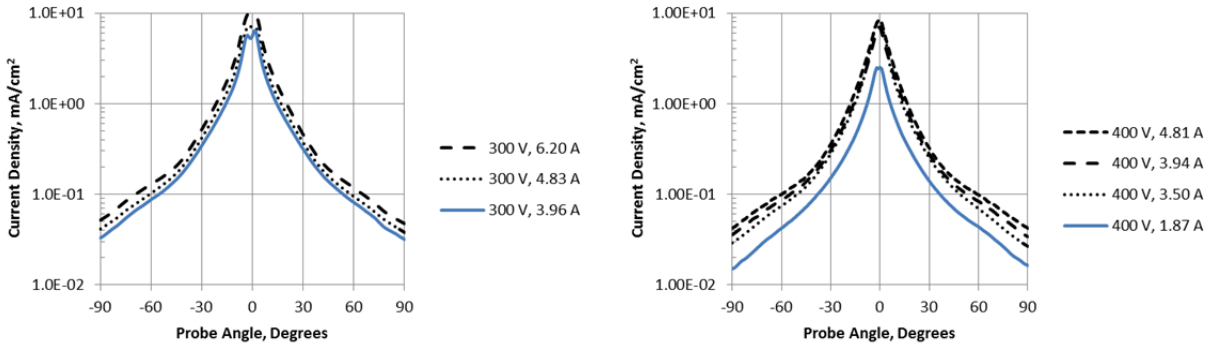

Figure 13. Krypton ion current density at 300 V and 400 V.

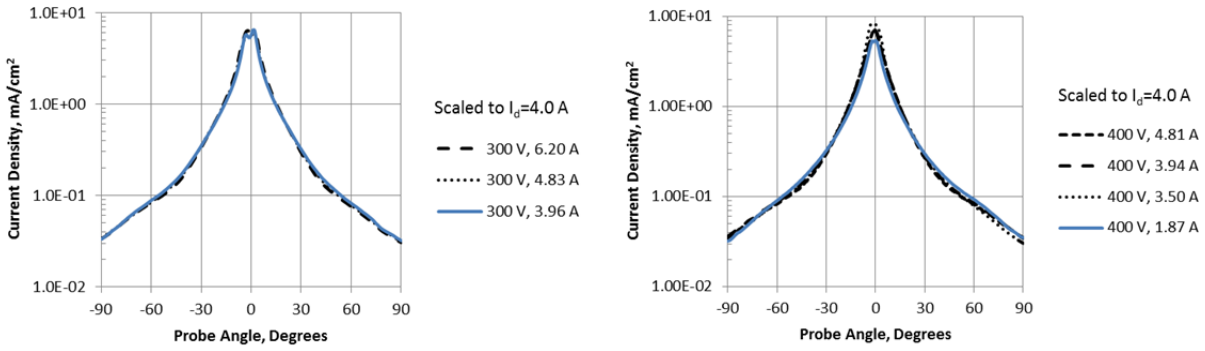

Figure 14. Krypton ion current density at 300 V and 400 V scaled to 4 A.

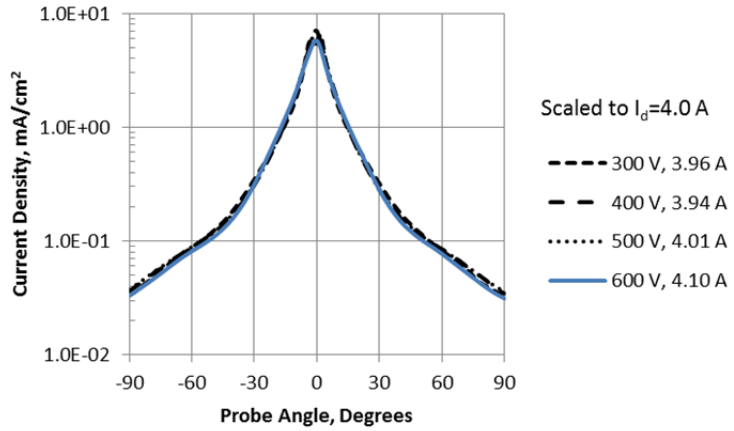

Figure 15. Scaled krypton ion current density at 300 V – 600 V.

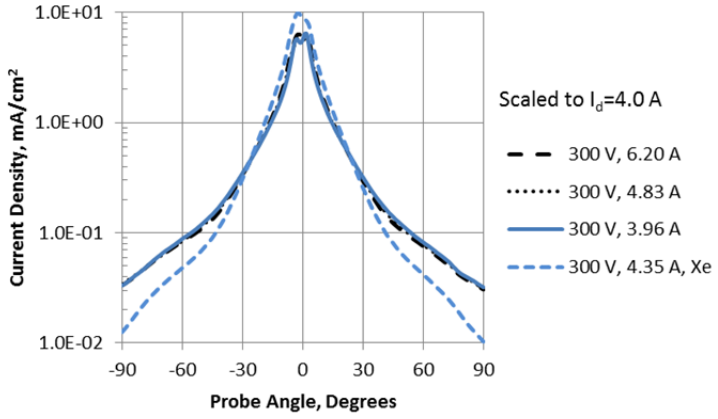

Figure 16. Scaled krypton and xenon ion current density at 300 V.

IV. Discussion

A. Krypton Performance Trends

Krypton efficiency varied with operating conditions, but generally increased with flow rate and discharge potential, peaking near 50%. The thruster was significantly more efficient with xenon.

Specific impulse was higher with krypton than with xenon at equivalent discharge conditions (P_d, V_d), but the increase was tempered by losses. To first order, the speed of an ion that has passed through the discharge is proportional to $\sqrt{V_d / M}$, where M is the ion mass. This suggests a 25% increase in I_{sp} when switching to krypton. The actual increase was closer to 10%. Still, per the rocket equation, a 10% gain in specific impulse means a 10% gain in overall spacecraft delta V for a given fuel load.

Chamber pressure was relatively high during krypton testing. However, xenon data taken at the Aerospace Corporation with the BHT-1500-E showed that specific impulse and efficiency are relatively constant with respect to chamber pressure when the cathode is center mounted. This indicates that the krypton performance data reported here are similar to what would be observed in-space.

The krypton data are also relevant to the BHT-1500-E. The measured efficiency of the xenon fueled BHT-1500-E at a background pressure of ~8 x 10^{-6} Torr was similar to the measured efficiency of the BHT-1500-C at a background pressure of ~ 1 x 10^{-5} Torr, as detailed in Table 3. This similarity should carry over to krypton. Figure 17 plots measured thruster efficiency for both thrusters and propellants, illustrating all at once the invariance of the BHT-1500-E xenon data with respect to background pressure, the similarity of the BHT-1500-E and BHT-1500-E xenon data, and the size of the efficiency loss associated with krypton in the BHT-1500-C.

Table 3. Performance of BHT-1500-C vs. BHT-1500-E with xenon at similar conditions (Data from Ref. 24).

Thruster	Gas	Power (Watts)	Discharge Potential (Volts)	Specific Impulse (s)	Efficiency (%)	P Background (Torr)
BHT-1500-E	Xe	1.5	300	1710	55.4	7.8E-06
		1.5	400	1878	51.8	6.0E-06
		1.8	300	1763	57.1	8.8E-06
		1.8	400	1942	53.6	7.1E-06
BHT-1500-C	Xe	1.6	300	1680	52.0	1.3E-05
		1.4	400	1890	51.5	1.1E-05
		1.9	300	1700	53.1	1.5E-05
		1.8	400	1970	54.3	1.0E-05

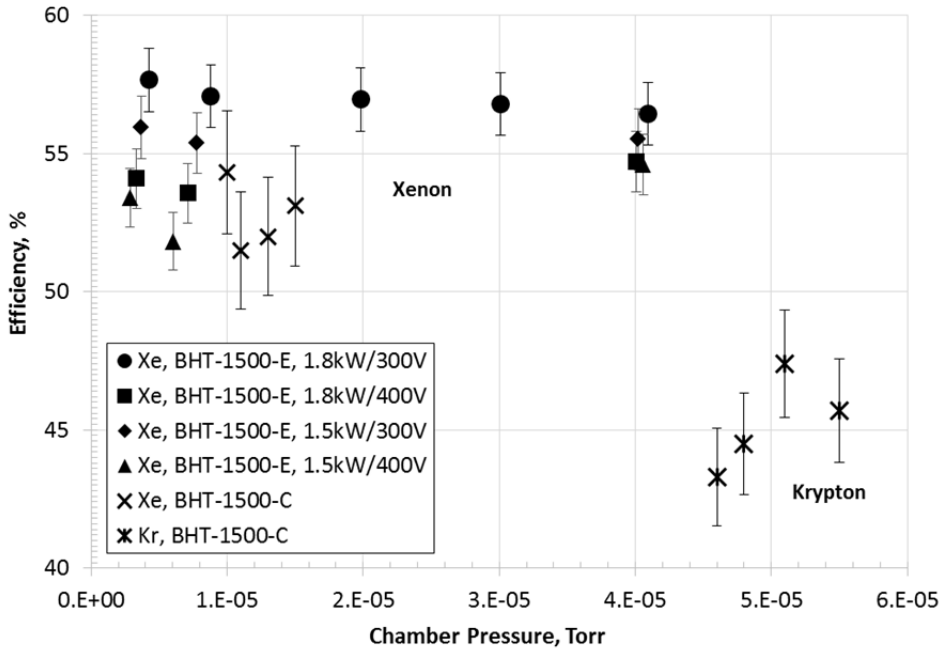

Figure 17. Center cathode efficiency of BHT-1500-E and BHT-1500-C with krypton and xenon (BHT-1500-E Data from Ref. 24).

B. Plume Divergence

The krypton plume shape showed little variation with respect to discharge potential or anode flow rate. Ion current density as a function of angle was essentially proportional to the discharge current.

Prior analysis of xenon plumes has shown that the ion flux at large angles is comprised almost entirely of charge exchange ions, many of which are produced when high energy ions collide with background neutrals.[27] It follows that the flux of krypton charge exchange ions was roughly proportional to discharge current.

Although the plume was considerably more divergent with krypton than with xenon, the krypton plume was measured at higher background pressure, and therefore the shape of the krypton plume was more affected by charge exchange collisions. The effects of background pressure may be partially removed by several methods. One is to extend the exponential portion of the central plume to ±90.[32] Plume current density decays with distance from the beam center at roughly an exponential rate, where the point of origin is well represented by the center of the thruster at radial distances more than four mean thruster channel diameters.[33] In Figure 18, the exponential portion of the 300 V krypton plume between $15 \le \theta \le 35$ degrees is extended to 90 degrees. The 300 V xenon plume is also shown, along with an extension from the exponential portion between $15 \le \theta \le 36$ degrees. With the exponential extrapolation, the krypton plume remains more divergent. A more accurate estimate of the in-space plume may be obtained if multiple sweeps are collected at different background pressures.[28,34]

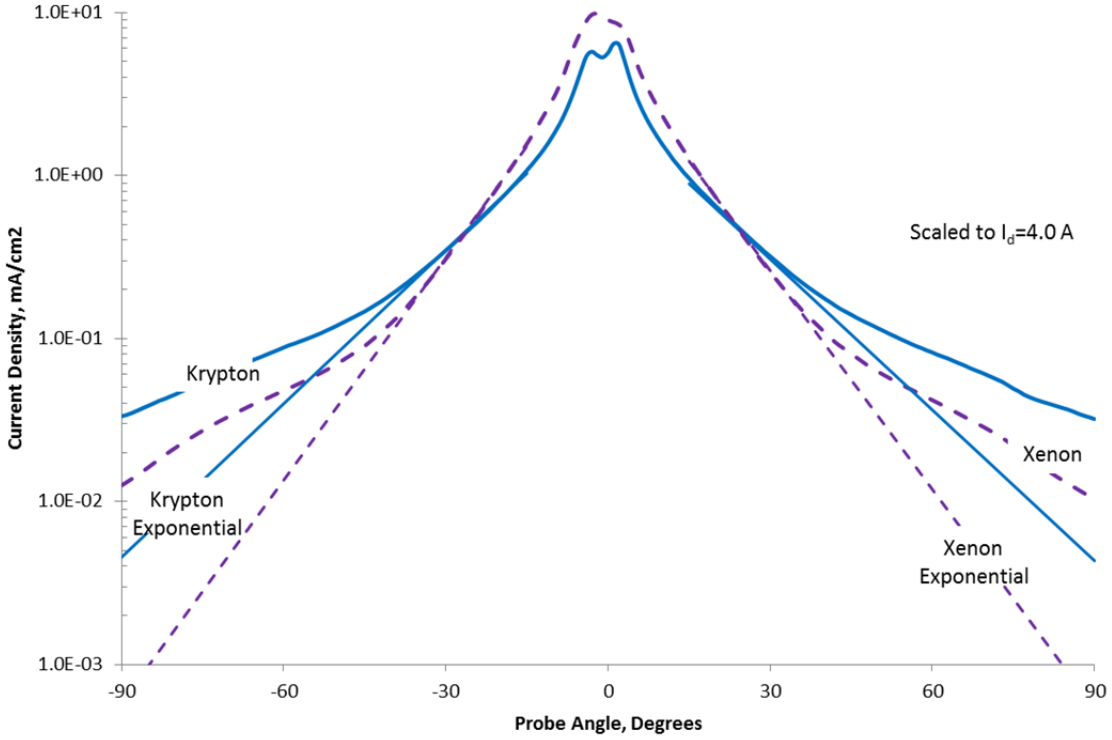

Figure 18. Plume current at 300 V for krypton and xenon.

C. Lifetime Considerations

Thruster and cathode lifetimes may be influenced by ion sputtering rates, which are different for krypton and xenon. Sputtering yield for krypton upon cathode keeper materials such as carbon and molybdenum may be higher. Sputter yields in the discharge channel will also be different. Kim reported lower borosil (BN-SiO_2 composite) sputter yield per Coulomb of charge at energies of interest.[35] However, limited life testing of the Fakel SPT-100 showed that erosion profiles progressed differently with Xe and Kr – not just at different rates.[16]

To minimize the impact of ion sputtering upon thruster lifetime, a thruster may be designed to eliminate channel erosion entirely at beginning of life. To accomplish this goal, a "magnetically shielded" version of the BHT-1500 was designed and built, retaining a center mounted cathode. The thruster was delivered to NASA's Jet Propulsion Laboratory (JPL) in 2015. It has not yet been tested with krypton.

The lifetime of the hollow cathode electron emitter may also be impacted by the use of krypton. The evaporation rate of the barium-calcium-aluminate mixture increases with temperature, which is influenced by internal plasma conditions.

V. Conclusions

A BHT-1500-C laboratory model with center mounted cathode was tested with krypton and xenon. The thruster was stable with both propellants. Cathode floating potential was similar with both propellants. The required magnetic field strength was lower with krypton, improving margin on the thruster design. At reference conditions, thruster efficiency was lower with krypton, but specific impulse was 8 – 10% higher. With krypton, specific impulse exceeded 2000 s at a discharge potential of 400 V, and thruster efficiency peaked near 50% at a discharge power of 2 kW. The krypton plume shape changed very little with operating conditions (thruster power, discharge current, discharge potential), and the shape was more divergent with krypton than with xenon. From these results, krypton appears to be a viable option for the flight model thruster, the BHT-1500-E.

Acknowledgments

The authors wish to acknowledge the Unites States Air Force for support under contract FA9300-06-C-1001.

References

[1]Grishin, S. D. and Leskov, L. V., *Electrical Rocket Engines of Space Vehicles*, Mashinostroyeniye, Moscow, 1989.

[2]Kim, V., "Main Physical Features and Processes Determining the Performance of Stationary Plasma Thrusters," *Journal of Propulsion and Power*, Vol. 14, No. 5, 1998, pp. 73 –743.

[3] Morozov, A., I., "The Conceptual Development of Stationary Plasma Thrusters," *Plasma Physics Reports*, Vol. 29, No. 3, 2003, pp. 235-250.

[4]Hruby, V., Monheiser, J., Pote, B., Freeman, C., and Connolly, W., "Low Power, Hall Thruster Propulsion System," *Proceedings of the 26th International Electric Propulsion Conference*, Electric Rocket Propulsion Society, IEPC 99-092, Kitakyushu, Japan, Oct 1999.

[5] Szabo, J., Pote, B., Paintal, S., Robin, M., Hillier, A., Branam, R., Huffman, R., "Performance Evaluation of an Iodine Vapor Hall Thruster", *Journal of Propulsion and Power*, Vol. 28, No. 4, 2012, pp. 848-857.

[6] Szabo, J., Robin, M., Paintal, S., Pote, B., Hruby, V., Freeman, C., "Iodine Plasma Propulsion Test Results at 1-10 kW," *IEEE Transactions on Plasma Science, Special Issue – Plasma Propulsion*, Vol. 43, No. 1, 2015, pp. 141-148.

[7]Szabo, J., Robin, M., Paintal, Pote, B., S., Hruby, V., "High Density Hall Thruster Propellant Investigations," *48th AIAA/ASME/SAE/ASEE Joint Propulsion Conference and Exhibit,* AIAA 2012-3853, July 2012.

[8] Szabo, J., Robin, M., Hruby, V., "Bismuth Vapor Hall Effect Thruster Performance and Plume Experiments," *Proceedings of the the 35th International Electric Propulsion Conference*, Electric Rocket Propulsion Society, IEPC 2017-25, Atlanta, GA, October 8 - 12, 2017

[9] *CRC Handbook of Chemistry and Physics*, 83rd Edition, CRC Press, Boca Raton, FL, 2002.

[10] Syage, J., "Electron-impact cross sections for multiple ionization of Kr and Xe," *Phys. Rev. A*, 46, 9, 1992, pp. 5666-5679.

[11]Hayes, T., Wetzel, R., Freund, R., "Absolute electron-impact-ionization cross-section measurements of the halogen atoms," *Physical Review A*, 35, 2, January 15, 1987, pp, 578-584.

[12]Tawara, H. and Kato, T., "Total and Partial Ionization Cross Sections of Atoms and Ions by Electron Impact," *Atomic Data and Nuclear Data Tables 36*, 1987, pp. 167-353.

[13]Welle, R., "Propellant Storage Considerations for Electric Propulsion," *Proceedings of the 22nd International Electric Propulsion Conference,* Electric Rocket Propulsion Society, IEPC 1991-107, Viarregio, Italy, Oct 14 – 17, 1991.

[14]Nakles, M., Barry, R., A Plume Comparison of Xenon and Krypton Propellant on a 600 W Hall Thruster," *Proceedings of the 31st International Electric Propulsion Conference*, Electric Rocket Propulsion Society, IEPC 09-115, Ann Arbor, Michigan, Sep 20 – 24, 2009.

[15]Hargus, W., Tango, L., and Nakles, M. "Background Pressure Effects on Krypton Hall Effect Thruster Internal Acceleration," *Proceedings of the 33rd International Electric Propulsion Conference*, Electric Rocket Propulsion Society, IEPC 2013-F, Washington, D.C., Oct 6-10, 2013.

[16]Nakles, M, Hargus, W., Delgado, J., and Corey, R., "A Performance and Plume Comparison of Xenon and Krypton Propellant on the SPT-100," *48th AIAA/ASME/SAE/ASEE Joint Propulsion Conference and Exhibit*, AIAA 2012-4116, Atlanta, GA, July – August 2012.

[17]Nakles, M., Hargus, W., Delgado, J., Corey, R., "A 205 Hour Krypton Propellant Life Test of the SPT-100 Operating at 2 kW," *Proceedings of the 33rd International Electric Propulsion Conference,* Electric Rocket Propulsion Society, IEPC-2013-347, Washington D.C., October 6-10, 2013.

[18]Kim, V., Popov, G., Kozlov, V., Skrylnikov, A., Grdlichko, D., "Investigations of SPT Performance and Particularities of it's Operation with Kr and Kr/Xe Mixtures," *Proceedings of the 27th International Electric Propulsion Conference*, Electric Rocket Propulsion Society, IEPC-01-065, Pasadena, CA, October 15 – 19, 2001.

[19]Bugrova, I., Morozov, A. Lipatov, A., Bishaev, M., Kharchevnikov, V., and M. V. Kozintseva, M., "Integral and Spectral Characteristics of ATON Stationary Plasma Thruster Operating On Krypton and Xenon," *Proceedings of the 28th International Electric Propulsion Conference*, Electric Rocket Propulsion Society, IEPC 03-366, Toulouse, France, Mar 17-21, 2003

[20]Linnell, J., Gallimore, A., "Efficiency Analysis of a Hall Thruster Operating with Krypton and Xenon," *Journal of Propulsion and Power*, Vol. 22, No. 6., 2006, pp. 1402 – 1412.

[21]Linnell, J. and Gallimore, A. , "Internal Plasma Structure Measurements of a Hall Thruster Using Xenon and Krypton Propellant", *Proceedings of the 29th International Electric Propulsion Conference,* Electric Rocket Propulsion Society, IEPC Paper 05-024, Princeton University, Oct - Nov 2005.

[22]Jacobson, D., Manzella, D., "50 kW Class Krypton Hall Thruster Performance," *39th AIAA/ASME/SAE/ASEE Joint Propulsion Conference and Exhibit*, AIAA 2003-4550, Huntsville, AL, July 20-23, 2003.

[23]Hofer, R., Johnson, L., Goebel, D., Wirz, R.., "Effects of Internally Mounted Cathodes on Hall Thruster Plume Properties," *IEEE Transactions on Plasma Science*, Vol. 36, No. 5, 2008, pp. 2004 – 2014.

[24]Diamant, K., Curtiss, T., Spektor, R., Beiting, E., Hruby, V., Pote, B., Kolencik, J., Paintal, S.., "Performance and Plume Characterization of the BHT-1500 Hall Thruster," *Proceedings of the 34th International Electric Propulsion Conference,* Electric Rocket Propulsion Society, IEPC-2015-69, Hyogo-Kobe, Japan July 4 – 10, 2015.

[25]Diamant, K., Liang, R., Corey, R., The Effect of Background Pressure on SPT-100 Hall Thruster Performance , *50th AIAA/ASME/SAE/ASEE Joint Propulsion Conference*, AIAA 2014-3710, Cleveland, OH, July 28-30, 2014.

[26]Szabo, J., Azziz, Y., "Characterization of a High Specific Impulse Xenon Hall Effect Thruster," *Proceedings of the 29th International Electric Propulsion Conference,* Electric Rocket Propulsion Society, IEPC 05-324, Princeton, NJ, Oct - Nov 2005.

[27]Azziz, Y., Martinez-Sanchez, J., Szabo, J., "Effect of Discharge Voltage on Plume Divergence of a High Specific Impulse Hall Thruster," 41st *AIAA/ASME/SAE/ASEE Joint Propulsion Conference and Exhibit*, AIAA-2005-4403, Tucson, AZ, July 10-13, 2005.

[28]Azziz, Y., Martinez-Sanchez, J., Szabo, J.,, "Determination of In-Orbit Plume Characteristics from Laboratory Measurements," 42nd *AIAA/ASME/SAE/ASEE Joint Propulsion Conference and Exhibit*, AIAA-2006-4484, Sacramento, CA, July 9-12, 2006.

[29]Azziz, Y., "Experimental and Theoretical Characterization of a Hall Thruster Plume," Ph.D. Dissertation, MIT Department of Aeronautics and Astronautics, June 2007.

[30]Rotter, J., "An Analysis of Multiple Configurations of Next-Generation Cathodes in a Low Power Hall Thruster," MS Dissertation, Air Force Institute of Technology, AIFT/GA/ENY/09-MO7, March 2009.

[31]Haag, T., "Thrust Stand for High-Power Electric Propulsion Devices," *Review of Scientific Instruments,* 62, 1991, pp. 1186-1191.

[32]McVey, J., Britt, E., Engelman, S., Gulczinski, F., Beiting, E., Pollard, J., Characteristics of the T-220ht Hall-Effect Thruster," *39th AIAA/ASME/SAE/ASEE Joint Propulsion Conference*, AIAA-2003-5158, Huntsville, AL, July 20-23, 2003.

[33]Brown, D., Gallimore, A., "Evaluation of facility effects on ion migration in a Hall Thruster plume," *Journal of Propulsion and Power*, Vol. 27, No. 3, 2011, pp. 573-585.

[34]Brown, D., Walker, M., Szabo, J., Huang, W., Foster, J., "Recommended Practice for Use of Faraday Probes in Electric Propulsion Testing," *Journal of Propulsion and Power,* Vol. 33, No. 3, 2017, pp. 582-613.

[35]Kim, V., Kozlov, V., Semenov, A., Shkarban, I., "Investigation of the Boron Nitride based Ceramics Sputtering Yield Under it's Bombardment by Xe and Kr ions," *Proceedings of the 27th International Electric Propulsion Conference*, Electric Rocket Propulsion Society, IEPC-01-073, Pasadena, CA, October 15 – 19, 2001.